Transactions on Engineering Sciences vol 39, © 2003 WIT Press, www.witpress.com, ISSN 1743-3533

CFD simulation of an HVOF process for the optimization of WC-Co protective coatings

C. Bartuli, F. Cipri, T. Valente & N. Verdone
Department of Chemical and Materials Engineering
University "La Sapienza", Rome, Italy

Abstract

Microstructured and nanostructured WC-Co composite coatings can be deposited by HVOF starting from commercial composite powders. However, the reduction in powder size of the ceramic reinforcement is responsible for a significant increase of WC reactivity, enhancing the decarburation phenomena taking place within the spraying torch, and potentially affecting the mechanical and tribological properties of the deposited coatings. In order to limit the thermal degradation of the reinforcement, it is therefore necessary to strictly control the main combustion parameters of the torch, such as composition, velocity and temperature of the combustion gases. Using a CFD code, thermo-chemical and gas-dynamic properties of the gas flow within an HVOF JP-5000 (Hobart Tafa Inc.) torch were simulated. Results of the simulation were used to reconstruct the thermo-chemical history of the powders during their residence in the gas stream.

1 Introduction

HVOF (High-Velocity Oxygen Fuel) is a thermal spray deposition process developed to produce dense, adherent and virtually defect-free coatings with high reproducibility at competitive cost [1]. A mixture of oxygen and fuel is continuously fed and combusted in the spraying torch, whose converging-diverging nozzle is designed to produce extremely high gas and particles velocities. The temperature attained by the particles in the combustion flame is relatively low, if compared to other thermal spray processes, such as plasma spray.

The combination of high velocity and low temperature allows to deposit coatings characterized by good cohesion and adhesion with the substrate, while reducing in principle of thermal degradation and/or oxidation of the particles.
Composite WC-Co coatings for wear resistant applications are typically deposited by HVOF [2]. Improved performance (higher surface hardness and better tribological properties) can be expected from the use of nanocrystalline coatings [3-5]. However, due to the higher reactivity and grain growth sensitivity of nanostructured ceramic reinforcements, the exposure to high temperature oxidizing flames must be minimized, while guaranteeing the formation of dense and homogeneous deposits [6]. A strict control of the main combustion parameters, and the ability of predicting composition, velocity and temperature of the combustion gases and of the particles within the jet is therefore of the utmost importance.
In the last years, several papers were dedicated to the simulation of HVOF processes using computational fluo-dynamical models (CFD) [7-10]. The present paper investigates the properties of gases and powders in a liquid fuel commercial HVOF Hobart Tafa JP-5000 gun, with the final aim of optimizing the spraying conditions for a nanostructured WC-15% Co composite powder.

2 Experimental methods

2.1 Materials and equipments

The spraying equipment used for the experimental campaigns in the present work is a liquid fuel JP-5000 Hobart-Tafa HVOF apparatus, burning a kerosene-oxygen mixture. The torch, essentially consisting of a kerosene injector, a combustion chamber and a convergent-divergent de Laval nozzle, is described in more details in the following paragraphs. All components are made of copper and water-cooled. A copper barrel is positioned at the end of the torch.
Standard operating conditions for the deposition of wear resistant WC-Co coatings were simulated in the present investigation. Oxygen mass flow was fixed at 2000 scfh (0.02125 kg/s); kerosene mass flow was set at 6.0 gph (0.00576 kg/s), 6.5 gph (0.00625 kg/s, stoichiometric conditions) and 7.0 gph (0.00679 kg/s). Barrels of different length (4", 8" and 12") were used to control the gas and particles flow at the exit of the torch.
Nanostructured WC-15% wt. Co powders (Nanocarb®, Union Miniere, NJ, USA) with a gaussian size distribution (average size 47 μm, 60% of the powders ∈ 30-60 μm, as characterized by laser granulometry (Malvern Mastersizer)) were used as feedstock material. Pressure and mass flow rate were of argon carrier gas were 446062 Pa and 10 l/min, respectively. Feed rate of the powders was 76 g/min.

2.2 Computational model

In order to solve the integral equations of momentum, energy and mass flow conservation and the auxiliary scalar equations describing turbulence, chemical reactions, species transport, etc., the 2D and 3D geometrical domains were

divided in finite discrete control volumes defining computational grids. The geometrical models and the reference grids were generated using a commercial pre-processor software (GAMBIT 1.3 [Fluent Inc. USA]), while all numerical simulations were carried out implementing the FLUENT 5.4.8 solver [Fluent Inc. USA] on a standard PC station.
The three basic equations of continuity (momentum, mass flow and energy) were solved using a segregated method allowing to iteratively integrate only one single equation for each finite volume over all the computational domain. The solution convergence of the analytical system was monitored by controlling normalized residuals. All solutions presented in this paper have residual values lower than 10^{-7} for mass flow and momentum equations and lower than 10^{-10} for energy equation of continuity and for all other scalar equations.

Gas-dynamical model

The SIMPLE algorithm (Semi-Implicit-Method for Pressure-Linked Equations) [11] was used to estimate the values of pressure and mass flow values on the faces of the individual cells starting from the central values of two adjacent cells. The k-ε model [15] (k representing the turbulent kinetic energy and ε its dissipation rate) was used to describe complete turbulence. Turbulent velocity and eddies scale length can be calculated solving two different transport equations:

$$\rho\frac{Dk}{Dt} = \frac{\partial}{\partial x_i}\left[\left(\mu + \frac{\mu_t}{\sigma_k}\right)\frac{\partial k}{\partial x_i}\right] + G_k - \rho\varepsilon - Y_M$$

$$\rho\frac{D\varepsilon}{Dt} = \frac{\partial}{\partial x_i}\left[\left(\mu + \frac{\mu_t}{\sigma_\varepsilon}\right)\frac{\partial \varepsilon}{\partial x_i}\right] + C_{1\varepsilon}\frac{\varepsilon}{k}\left(G_k + C_{3\varepsilon}G_b\right) - C_{2\varepsilon}\rho\frac{\varepsilon^2}{k}$$

where ρ is the fluid density, μ and μ_t are viscosity and turbolent viscosity, G_k is the rate of generation of k caused by the average flow velocity, Y_M represents the dissipation caused by flow compressibilty, $C_{1\varepsilon}$, $C_{2\varepsilon}$ and $C_{3\varepsilon}$ are empyrical constants and σ_k and σ_ε are Prandtl numbers for k and ε.
Turbuent flows are influenced by the presence of walls. The flow field beside the wall was described as the sum of a viscous substrate (high molecular viscosity, laminar conditions), a transition layer (molecular and turbulent viscosity have the same order of magnitude) and a turbulent layer (high turbulence caused by high velocity gradient) [12]. "Non equilibrium wall function" [13] can model the viscous substrate and the transition layer using modified Launder & Spalding functions in order to account for the high velocity and pressure gradients and for heat exchange.

Chemistry model

In HVOF torches the combustion rate is much faster than turbulent dynamics. A *Finite rate chemistry* [14] model can be employed to solve the transport equations for reagents and products. In order to minimize the need for

computational resources, chemical equilibrium is assumed at all times, and the reaction rates are evaluated by Eddy Dissipation Concept (EDC) [15], a general method used to analyse the influence of turbulence phenomena on the chemistry of combustion flames.
Inside the combustion chamber, temperatures can be higher than 2000 K, and to obtain the correct adiabatic flame temperature it is therefore necessary to account for the dissociation of the products. Equilibrium stoichiometric coefficients of molecular and dissociated species were calculated at the experimental pressure (about 8 bar) using a commercial monodimensional chemical code (GASeq: chemical equilibria for perfect gases, (free available software, release 0.63). For 6.5 gph of kerosene they can be resumed by the following reaction:

$$4C_{12}H_{23}+71O_2 \Leftrightarrow 12.4O_2+5.74O+31.84H_2O+19.62CO_2+28.38CO+12OH+4.76H+5.78H_2$$

The local mass fractions of individual species were computed by solving scalar convection-diffusion equations. The reaction kinetic constant in the trasport equations was evaluated by EDC. Transport equations were solved for all individual components; thermal properties of the mixture were calculated, for each temperature, according to the law of mixtures.

Particles modeling

The presence of a discrete phase in the form of solid spherical particles characterized by a known size distribution was also simulated in a Lagrange reference using the FLUENT solver. The trajectories of the particles and their thermo-chemical interaction with the turbulent combustion stream was modeled in the hypothesis of negligible interaction among the particles (diluted solid phase). Calculations were based on the fundamental equations of force balance, convective and radiative heat exchange and mass tranfer for the individual particles.

2.3 Computational domain, grid geometry and boundary conditions

In Figure 1 the geometrical model of the combustion chamber and adjacent elements is described. The model was reconstructed by disassembling, sectioning and measuring all torch components. Four main parts can be identified: kerosene injector, combustor, de Laval nozzle and feed pipe. The kerosene flow enters the torch trough a 1.3 mm diameter duct, and is atomized by the oxygen stream entering from a coaxial pipe (2.0 mm internal diameter, 5.6 mm external diameter). The total number of cells in the grid is 14085: cells spacing was design to optimize the simulation of the most important physico-chemical phenomena, such as heating exchange on the walls, chemical reactions between the species, supersonic transition, etc..

Transactions on Engineering Sciences vol 39, © 2003 WIT Press, www.witpress.com, ISSN 1743-3533

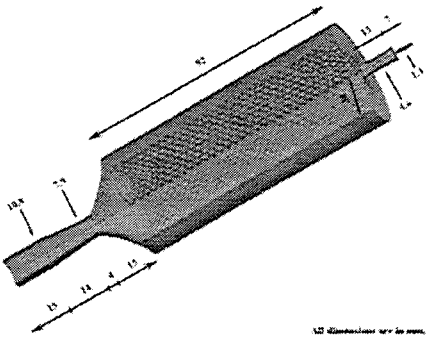

Figure 1: Geometrical model of kerosene injector, combustion chamber, de Laval nozzle and feed pipe

Temperature of the solid walls was fixed at 58°C, on the basis of the results of temperature measurements of the cooling water out the torch. The flow field was initialized with a 200 m/s velocity and a 2000 K temperature.
Figure 2 shows the grid used to reconstruct the flow field in the external domain in the case of the 4" barrel.

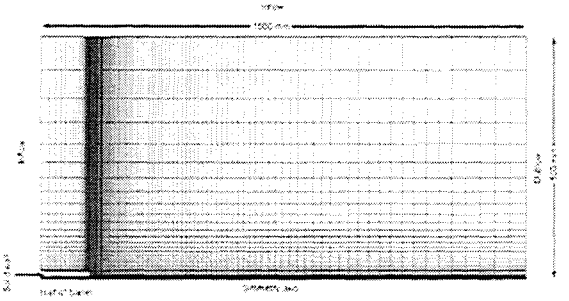

Figure 2: 2-dimensional geometrical reconstruction of the 4" barrel (bottom part of the chart) and of the external flow field.

Geometrical boundaries were positioned at a large distance from the exit zone of exhaust gases, in order to reconstruct the real conditions without deforming the external flow field. Total number of cells is 24984 for the 12" barrel, 22457 for the 8" barrel and 20531 for the 4" barrel. Initial conditions were calculated from the results of the simulation of the adjacent feed pipe at 6.5 gph. The external air pressure was fixed at 101325 Pa, and the external temperature at 300 K. Temperature of the copper walls of the 4", 8" and 12" barrels were as 59, 63 and 67 °C, respectively. The solution was initialized applying to the whole computational domain an initial velocity of 1000 m/s and a temperature of 300K. To avoid solution divergency, the simulation of chemical reactions in the first iterative steps is avoided, and the problem is initially approached using a cold

flow strategy: the simulation of the flow reactivity is introduced as a further step when residuals are stabilized.
The two powders injectors are inserted at the end of the feed pipe: to reconstruct the particles behaviour in the barrels, a 3-dimensional grid formed by tetrahedral elements was designed, characterized by two planes of symmetry (Figure 3). Flow conditions calculated for the combustion chamber outlet at 6.5 gph were used at the barrel inlet. Particles enter through the injectors, transported by a flow of argon carrier gas (446062 Pa, 10 l/min). The total number of tetrahedral cells is 27000 for the 4" barrel, 41000 for the 8" barrel and 55000 for the 12" barrel. Initial temperature of the jet is 1500 K, and initial velocity is 1500 m/s.

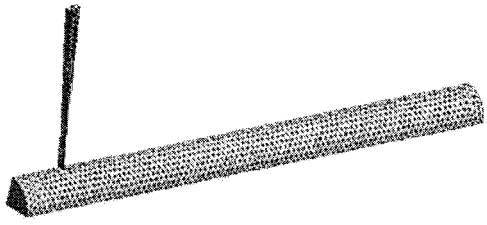

Figure 3: 3-dimensional geometrical recontruction (tetrahedral elements) of the feed pipe and barrel (quarter) and of one of the powders injectors (half).

3 Results and discussion

3.1 Combustion chamber

Figure 4a shows the static temperature profile along the torch centerline, for three different compositions of the mixture. The model takes into account the dissociation of combustion products. Calculated peak temperatures are 3287 K (6.0 gph), 3207 K (6.5 gph) and 3120 K (7.0 gph), slightly lower than those calculated by GASeq for chemical equilibrium, taking into account that the system is not adiabatic: the calculated dissipated power for the cooling of the combustor is 48.7 kW at 6.5 gph. Results are confirmed by experimental evidence. The average value of static temperature calculated on the section positioned at the end of the combustion chamber is 2435 K (6.5 gph): combustion is not completed within the combustor, due to low turbulence and low injector efficiency. The higher turbulence in the de Laval nozzle finally allows the reaction to reach the thermodynamical equilibrium.
The static pressure profile along the centerline axis is shown in Figure 4b. Steady state combustion is an isobaric process, and the pressure in the chamber is therefore only correlated with the total mass flow of the gases inside the torch. Experimental measurements confirm a static pressure of 825300 Pa at 6.5 gph at the chamber inlet.

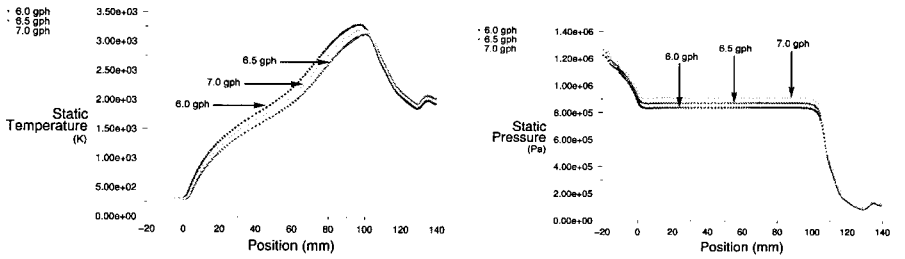

Figure 4: Static temperature and static pressure profiles along the torch centerline, for three different compositions of the mixture (kerosene flow rates of 6.0, 6.5 and 7.0 gph).

An increase of the mass flow of the reactant species corresponds to an increase of the pressure and, consequently, of the kinetic energy of the gas at the exit of the nozzle. Figure 5 illustrates the variation of the gas velocity along the torch axis as a function of kerosene mass flow. The sudden decrease of gas velocity at the end of the divergent corresponds to the connection between the divergent and the feeder: the presence of a sharp edge (6°) generates an abrupt change in the direction of the flow, with the production a zone of high turbulence. The highest velocity calculated in the streamline is 1856 m/s (for 7.0 gph).
In Table 1 the average values of the main gasdynamical properties of the flow in three important sections of the torch are resumed for the three mixture compositions.

3.2 Barrel and external flow field

The barrel is a constant section copper pipe where a compressible reactive mixture flows, exchanges heat and interacts with the walls. Surface roughness induces local modifications of gas velocity and, consequently of temperature and pressure. The friction effect (Fanno) stabilizes the flow in sonic conditions; the velocity magnitude at the barrel inlet is about Mach 2 (supersonic) and the Fanno effect leads to a reconversion of kinetic energy into pressure enthalpy, with a decrease of velocity and the formation of a boundary layer that reduces the effective barrel cross-section.
In a duct with ideal smooth walls, a supersonic stream is decelerated when heated by an external source and accelerated when cooled (Raleigh flow). In the barrel, Fanno and Raleigh flows give opposite effects: the roughness of the walls decreases the velocity and increases temperature and pressure while the water cooling of the walls increases the velocity of the jet reducing its temperature and pressure. The temperature decreases along the barrel (see Figure 6a) because the recombination of the dissociated species and the Fanno effect do not produce a sufficient amount of heat to contrast the Raleigh effect.

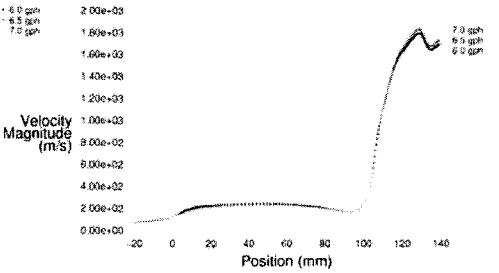

Figure 5: Gas velocity profile along the torch centerline (kerosene flow rates of 6.0, 6.5 and 7.0 gph).

Table 1: Average values of the main properties of the gas flow in three sections of the torch for three mixture compositions.

	Combustor outlet	Divergent outlet	Outlet
Static pressure (Pa)	839581 (6.0 gph) 873491 (6.5 gph) 908983 (7.0 gph)	108501 (6.0 gph) 113395 (6.5 gph) 118638 (7.0 gph)	114299 (6.0 gph) 119346 (6.5 gph) 124949 (7.0 gph)
Axial velocity (m/s)	51 (6.0 gph) 51 (6.5 gph) 50 (7.0 gph)	1652 (6.0 gph) 1687 (6.5 gph) 1718 (7.0 gph)	1588 (6.0 gph) 1622 (6.5 gph) 1653 (7.0 gph)
Mach number	0.047 (6.0 gph) 0.046 (6.5 gph) 0.046 (7.0 gph)	1.895 (6.0 gph) 1.890 (6.5 gph) 1.883 (7.0 gph)	1.823 (6.0 gph) 1.819 (6.5 gph) 1.811 (7.0 gph)
Static temperature (K)	2425 (6.0 gph) 2435 (6.5 gph) 2433 (7.0 gph)v	1824 (6.0 gph) 1868 (6.5 gph) 1903 (7.0 gph)	1818 (6.0 gph) 1863 (6.5 gph) 1902 (7.0 gph)

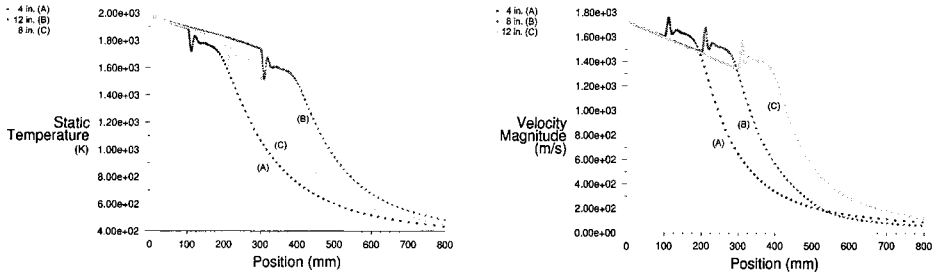

Figure 6: Static temperature (a) and velocity (b) profiles of the gas along the barrel and in the external field (barrel length of 4"(A), 8"(B) and 12"(C)).

A surface roughness R_a of 0.004 mm was selected for the present simulation. The dissipated power used to cool the barrel was calculated with a maximum relative error of about 5%.

The results of the simulation of the stream velocity (Figure 6b) show a decrease of the gas velocity towards the exit for all barrel lengths: it is therefore evident that the Fanno effect has a stronger influence on velocity than the Raleigh effect. However Fanno and Raleigh phenomena are not linear and it is not possible to compute a linear combination of the two effects.

The JP-5000 nozzle, in the operating conditions, is underexpanded and the static pressure rising from the divergent exit is higher than the atmospheric pressure. Figure 7 shows the absolute static pressure calculated at the domain centerline as a function of axial distance. Sudden pressure changes, characteristic of HVOF conditions, are formed as a consequence of the interaction of the oblique shock waves originated at the barrel exit, with the emission of visible light and are known as "shock diamonds".

The variation of the atomic oxygen mass fraction along the jet centerline for the 4" barrel is also illustrated in Figure 8, as a particular example.

In Table 2 the average values of the main properties of the flow in the barrel are resumed for the three barrel lengths.

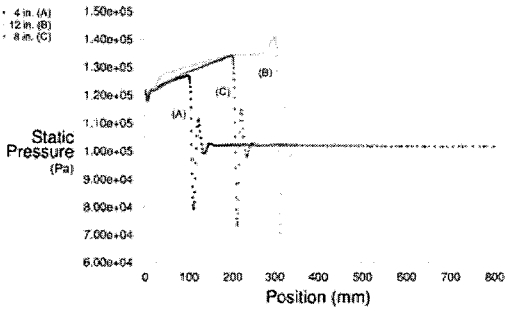

Figure 7: Variation of the static pressure along the jet centerline (barrel length of 4"(A), 8"(B) and 12"(C)); sudden pressure changes correspond to the formation of "shock diamonds".

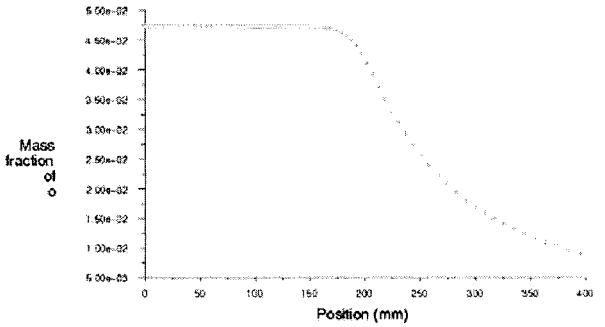

Figure 8: Variation of the atomic oxygen mass fraction along the jet centerline for a 4" barrel.

Table 2: Average values of the main properties of the gas in barrels of different length

	4" barrel	8" barrel	12" barel
Total heat dissipation (W)	-12157	-21522	-30382
Static pressure (Pa)	124998	131096	135498
Axial velocity (m/s)	1483	1351	1230
Mach number	1.702	1.586	1.478
Static temperature (K)	1782	1699	1617

3.3 Powders

The distributions of temperature and velocity of the powders were calculated in the combustor+nozzle section, in the barrel and at the exit of the torch.
Axial values of velocity and temperature in the barrel and in the external field are summarized in Figure 9 for the three different barrel lengths. The final sections of the barrels (4", 8" and 12") are indicated in the plots as dotted grey lines. The figure gives important indications about the selection of the best barrel to be used for a given spraying distance: optimal spraying conditions, identified by the maximum temperature and velocity of the particles compatible with the integrity of the substrate, can be identified, in the present case, as a spraying distance of about 300-400 mm from the exit of the barrel with a barrel length of 8 inches.
Finally, the simulation of particles traces coloured by particles temperature is illustrated in Figure 10 for a total distance from the initial section of the 12" barrel of 150 cm. The combination of temperature and trajectories spreading data is of fundamental importance for the evaluation of the deposition efficiency of the powders for substrates located at various distances from the torch.

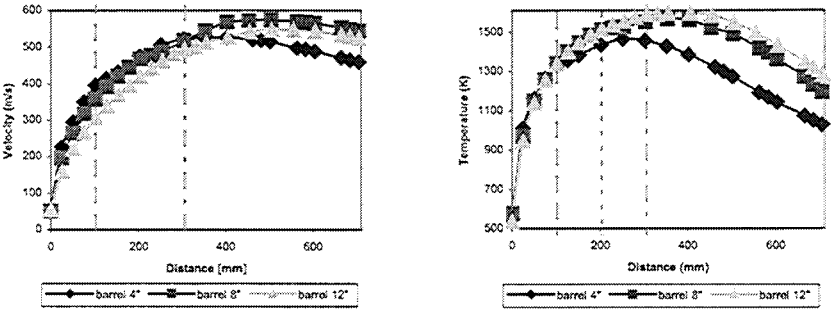

(a) (b)

Figure 9: Simulation of the average particles axial velocity (a) and temperature (b) as a function of the distance from the initial section of the barrel for three different barrel lengths.

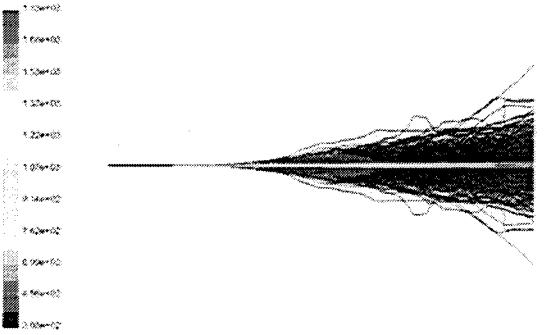

Figure 10: Simulation of the particles temperature and trajectories at the 12" barrel exit.

4 Conclusions

The computational modeling of the complex phenomena that take place in a high velocity oxygen-kerosene spraying torch was approached by assuming simplified physical and chemical conditions for the combustion flame and for the solid particles in the torch and in the external field. Results of the simulation appear consistent with a number control parameters that were monitored during spraying, such as the power disperded for water-cooling of the torch.
Calculated properties of the powders (mainly in terms of temperature and velocity) and of the gas (composition of the mixture) were used to confirm the

selection of the best operating conditions for the deposition of conventional and nanostructured WC-Co coatings, requiring the use of the lowest temperature and the highest velocity of the particles (to guarantee limited growth of the nano-grain and low decarburation of the reinforcement) compatible with the built up of a coherent coating endowed with sufficient adhesion to the substrate and, possibly, with an adequate deposition efficiency [6]. The optimal compromise for WC-Co composite particles is represented by the use of an 8" barrel, allowing particles velocities of 572 m/s with a maximum temperature of 1568 K, and by a spraying distance of about 200-300 mm from the final section of the barrel.

References

[1] Fauchais, P.,. Vardelle, A.M, Dussoubs, B., "Quo Vadis Thermal Spraying?", in "Thermal Spray 2001: New Surfaces for a New Millennium", C.C. Berndt, K.A. hor, E. Lughscheider Eds., ASM International, Materials Park, OH, USA, pp.1-32, 2001.

[2] De Barro, J.A, Dorfman, M.R, in "Thermal Spraying: current status & future trends", A.Ohmori, Ed, High Temperature Soc. of Japan, Osaka, Japan, pp.651-656, 1995.

[3] Gusev A.I., *Physics,* **41 (1)**, 49-76 1998.

[4] Gartner, F., Bormann, R., Klassen, T., Kreye, H., Mitra, N., *J. Metast. Nano. Mat.,* **8**, pp.933-940, 2000.

[5] Gell, M., *Mat. Sci. Eng.,* **A 204**, pp.246-251, 1995.

[6] Bartuli, C., Valente, T., Cipri, F., Bemporad, E., Nanostructured Wear Resistant WC-Co Coatings Deposited by HVOF, *Proc. of the 13th IFHTSE/ASM Surface Engineering Congress 2002,* in press.

[7] Oberkampf, W.L., Talpallikar, M., Analysis of High-Velocity Oxygen-Fuel (HVOF) Thermal Spray Torch Part 1: Numerical Formulation, *Journal of Thermal Spray Technology*, **5 (1)**, pp. 53-68, 1996.

[8] Gu, S., Eastwick, C.N., Simmons, K.A., McCartney, D.G., Computational Fluid Dynamic Modeling of Gas Flow Characteristics in a High-Velocity Oxy-Fuel Thermal Spray System, *Journal of Thermal Spray Technology*, **10 (3)**, pp. 461-469, 2001.

[9] Sakaki, K., Shimizu, Y., Effect of the Increase in the Entrance Convergent Section Length of the Gun Nozzle on the High-Velocity Oxygen Fuel and Cold Spray Process, *Journal of Thermal Spray Technology*, **10 (3)**, pp. 487-496, 2001

[10] Yang, X., Eidelman, S., Numerical Analysis of a High-Velocity Oxygen-Fuel Thermal Spray System, *Journal of Thermal Spray Technology*, **5 (2)** 1996.

[11] Zucker, R.D., *Fundamentals of Gasdynamics,* Matrix Pub Lishers Inc.: Chesterland, OH, pp. 235-310, 1977

[12] Anderson Jr., J.D., *Computational Fluid Dynamics,* McGraw Hill: USA, pp.49-74, 1995.

[13] George, W.K., Arndt, R., *Advances in Turbulence*, Hemisphere Pub. Corp.: New York, London, pp. 79-88, 1989.

[14] Turns, S.R., *An Introduction to Combustion,* Mc Graw Hill: USA, pp. 372-375, 1996.

[15] Khalil,E.E., *Modelling of furnaces and Combustors*, Abacus Press, pp.27-29, 1982.

[16] Lentini, D., Jones, W.P., Numerical Simulation of nonpremixed Turbulent Flow in a Dump Combustor, *AIAA/SAE/ASME/ASEE 26th Joint Propulsion Conference 1990,* AIAA, Washington, D.C. 20020 USA, pp.1-8, 1990

[17] Cheng, D., Trapaga, G., McKelliget, J.W., lavernia, E.J., Mathematical Modeling of High Velocity Oxygen Fuel Thermal Spraying: An Overview, *Key Engineering Materials,* **197**, pp.1-26, 2001.